Comparison of ITRF2014 station coordinate input time series of DORIS, VLBI and GNSS

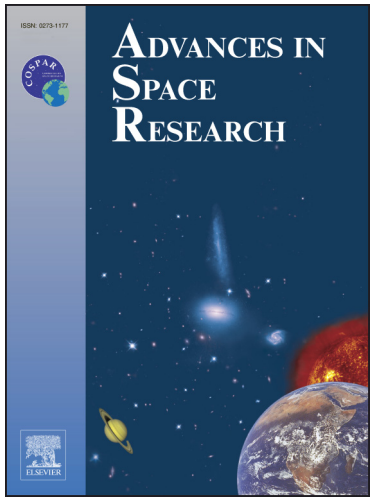

Comparison of ITRF2014 station coordinate input time series of DORIS, VLBI and GNSS

Vincenza Tornatore, Emine Tanır Kayıkç ı, Marco Roggero

PII: S0273-1177(16)30375-1
DOI: http://dx.doi.org/10.1016/j.asr.2016.07.016
Reference: JASR 12833

To appear in: *Advances in Space Research*

Received Date: 9 July 2015
Revised Date: 7 July 2016
Accepted Date: 11 July 2016

Please cite this article as: Tornatore, V., Kayıkç ı, E.T., Roggero, M., Comparison of ITRF2014 station coordinate input time series of DORIS, VLBI and GNSS, *Advances in Space Research* (2016), doi: http://dx.doi.org/10.1016/j.asr.2016.07.016

Comparison of ITRF2014 station coordinate input time series of DORIS, VLBI and GNSS

Vincenza Tornatore[1], Emine Tanır Kayıkçı[2], Marco Roggero[3]

[1]Politecnico di Milano, Dipartimento di Ingegneria Civile e Ambientale (DICA), Piazza Leonardo da Vinci 32, I-20133 Milano, ITALY, Email: vincenza.tornatore@polimi.it

[2]Karadeniz Technical University, Department of Geomatics Engineering, T-61080 Trabzon, TURKEY, Email: etanir@ktu.edu.tr

[3]Politecnico di Torino, Dipartimento di Architettura e Design (DAD), Viale Mattioli 39, I-10125 Torino, ITALY, E-mail marco.roggero@polito.it

Abstract

In this paper station coordinate time series from three space geodesy techniques that have contributed to the realization of the International Terrestrial Reference Frame 2014 (ITRF2014) are compared. In particular the height component time series extracted from official combined intra-technique solutions submitted for ITRF2014 by DORIS, VLBI and GNSS Combination Centers have been investigated.
The main goal of this study is to assess the level of agreement among these three space geodetic techniques. A novel analytic method, modeling time series as discrete-time Markov processes, is presented and applied to the compared time series.
The analysis method has proven to be particularly suited to obtain quasi-cyclostationary residuals which are an important property to carry out a reliable harmonic analysis. We looked for common signatures among the three techniques. Frequencies and amplitudes of the detected signals have been reported along with their percentage of incidence. Our comparison shows that two of the estimated signals, having one-year and 14 days periods, are common to all the techniques. Different hypotheses on the nature of the signal having a period of 14 days are presented.
As a final check we have compared the estimated velocities and their Standard Deviations (STD) for the sites that co-located the VLBI, GNSS and DORIS stations, obtaining a good agreement among the three techniques both in the horizontal (1.0 mm/yr mean STD) and in the vertical (0.7 mm/yr mean STD) component, although some sites show larger STDs, mainly due to lack of data, different data spans or noisy observations.

1. Introduction

The International Terrestrial Reference Frame (ITRF), established and maintained by the International Earth Rotation and Reference Systems Service (IERS), was adopted by the International Association of Geodesy (IAG) and the International Union of Geodesy and Geophysics (IUGG) in 1991. From ITRF2005 to the version ITRF2008 (Altamimi et al., 2011) the ITRF solutions have combined the station position and Earth Orientation Parameter (EOPs) time series from the four main space geodesy techniques: Very Long Baseline Interferometry (VLBI), Satellite Laser Ranging (SLR), Global Navigation Satellite System (GNSS), and

Doppler Orbitography and Radio-positioning Integrated by Satellites (DORIS), as well as terrestrial measured local ties at co-location sites (Altamimi et al., 2007).
Due to developments and progress for all the four space geodetic techniques a new call for participation for the computation of the new realization of ITRF (ITRF2014) was published (see http://itrf.ensg.ign.fr/ITRF_solutions/2013/CFP-ITRF2013-27-03-2013.pdf). Analysis Centers (ACs) belonging to individual geodetic services of the IAG: the International DORIS Service (IDS), the International Laser Ranging Service (ILRS), the International VLBI Service for Geodesy and Astrometry (IVS) and the International GNSS Service (IGS) reprocessed solutions according to common guidelines and improved models conforming with the IERS Conventions 2010, including updates posted at (http://tai.bipm.org/iers/convUPdt/convUPdt.html). In the Call for Participation, each AC was asked not to apply geophysical fluid loading effect corrections because the models are not commonly specified in the IERS Conventions. The use of a unique loading model provided by the IERS Global Geophysical Fluid Center (GGFC) was envisaged during the ITRF generation, though it was not applied. Non-tidal loading corrections were applied because of hydrology and ocean circulation according to their relevance.
Each official Combination Centers (CCs) belonging to each of the four IAG services computed combination of single technique AC solutions and submitted them to the IERS Central Bureau and the ITRS Center in the form of weekly or daily SINEX (Solution INdependent EXchange format).
Three official ITRS Combination Centers are responsible for the inter-technique computation of ITRS realizations, they are currently maintained by the following institutions: Institut Géographique National (IGN), Deutsches Gedätisches Forschungsinstitut- Technische Universität München (DGFI-TUM) and Jet Propulsion Laboratory (JPL). The official ITRF2014 solution computed by ITRS Center at IGN is available at http://itrf.ign.fr/ITRF_solutions/2014/.

The single technique combined solutions reprocessed for ITRF2014 constitute an important large and homogeneous data set. In order to reveal common signatures among space geodetic techniques we investigated the site position time series extracted from combined solutions submitted by three CCs belonging to IDS, IVS and IGS (official ILRS results were not available at the time of this study therefore SLR technique is not considered in this work).
The strategy we applied to analyze the station position time series is based on a state–space model of the time series (Commandeur and Koopman, 2007) that consists of a measurement equation relating the observed data to a state vector and a Markovian transition equation that describes the evolution of the state vector over time. State space models are defined and then solved by a Kalman filter (KF) plus smoothing determining the optimal estimates of the state vector at single epochs and therefore enabling estimates of signals constituents variable in time. Using this approach we first detected, estimated, tested and removed the time series discontinuities, then we modeled the non-linear and non-periodic long term signal.
For a number of reasons, coordinate time series derived from space geodetic data present discontinuities leading to non-homogeneity in the time series. Therefore discontinuities must be detected and removed prior to the estimation of trends and periodic effects in the coordinate time series. Several studies were carried out in the last decade, for example different solutions were proposed for automatic research of discontinuities and outlier removal (Hefty, 2001; Johansson et al., 2002; Kleijer, 2002; Perfetti, 2006; Roggero, 2012; Gazeaux et al., 2013). The noise characteristics of the time series were examined by different researchers (Williams, 2003; Tesmer et al., 2009; Woppelmann et al., 2009). The presence of temporal correlations and their effect on the estimation of position and velocity precision were also checked (Blewitt & Lavallée, 2002; Collilieux et al., 2007).

Using our approach that models stochastically time series within a KF framework, we obtained quasi-cyclostationary residuals. Processes in nature are called cyclostationary when they arise from periodic phenomena although they are not periodic functions of time and give rise to random data whose statistical characteristics vary periodically with time (Gardner et al., 2006). They are very important processes since cyclostationarity is a key property to detect reliable periodic signals through harmonic analysis. However for space geodetic coordinate time series, full cyclostationarity, theoretically required by harmonic analysis, cannot be achieved due to heteroskedasticity, i.e. non-uniform accuracy of the observations with respect to time.

Another problem for harmonic analysis on space geodetic time series is that they are often unevenly sampled. Several methods for time series frequency analysis are proposed in literature to detect periodic behaviors also considering the irregular sampling. These studies include the use of wavelets (Ding et al., 2005), periodograms (Ray et al., 2008), and Lomb periodograms (Scargle, 1982). Analogous approaches were developed by Petrov & Ma (2003), Blewitt & Lavallée (2002), Mao et al., (1999), Titov & Yakovleva (2000), and Langbein & Johnson (1997).

In this work, harmonic analysis was carried out on the geodetic discrete irregular sampled time series residuals by using the software Frequency Analysis Mapping On Unusual Sampling (FAMOUS) developed by Mignard (2005).

The objective of this paper is to present all the steps we have carried out to apply an innovative and effective method to model reprocessed input time series for ITRF2014. Our method was homogeneously applied to the whole set of data and succeeded to reveal common residual periodic signals among three space geodetic techniques: DORIS, VLBI and GNSS. The approach demonstrated to be also a useful tool to estimate reliable velocities.

The paper is organized as follows: the time series modeling and the characteristics of the investigated data sets are described in Section 2. The procedure employed to estimate the jumps or discontinuities in the time series is presented in Section 3. Once the signal jumps, the discontinuities and outlier are removed, the methodology applied to estimate a long-term signal is introduced in Section 4 together with some real examples. The algorithms employed in the FAMOUS software, used for harmonic analysis, are briefly outlined in Section 5. In addition, the signals identified for each technique together with their percentage of occurrence are presented in three subsections. Interpretations and hypothesis on the nature of the signals detected for each technique are also discussed.

For all the DORIS stations co-located with VLBI and GNSS, a detailed analysis is carried out and described in Section 6. The estimated horizontal and vertical velocities for each technique at co-located sites are also reported. Some anomalies found for particular sites are presented and discussed. Finally, the conclusions are drawn and an outlook is provided in Section 7.

2. Time series data set and modeling

In this paper we analyze the NEU (N, E, and Up) time series, extracted from the IDS, IGS and IVS combined SINEX solutions submitted to the IERS for ITRF2014 computation. Each set of solutions is the result of intra-technique combination of the respective ACs: six contributed to the IDS solution, nine to the IVS, and eight to the IGS. The time series have different time spacing: weekly for IDS, daily for GNSS and session-wise for VLBI.

The solutions contain the full history of IDS, IGS and IVS data collected by the respective global tracking networks. The data of 71 sites back to 1993 were reprocessed by IDS, the data

for 1845 sites back to 1994.0 by IGS and the data of 159[1] sites back to 1979 were processed by IVS.
The main characteristics of three solutions analyzed in the present work, (namely IDS, IGS and IVS time series) are summarized in Table 1, other details can be found in paragraphs 5.1, 5.2 and 5.3.

Table 1: Analyzed time series derived by the IDS, IGS and IVS intra-technique combined solutions submitted for ITRF2014 realization

Time Series	**DORIS**	**GNSS**	**VLB I**
Series number	IDS02	REPRO2	ivs2014a
Web address	ftp://cddis.gsfc.nasa.gov/doris/products/stcd/ids16wd02	ftp://igs-rf.ensg.eu/pub/repro2	ftp://ivs.bkg.bund.de/pub/vlbi/ITRF2014/daily_sinex/ivs2014a
Reference Frame	ITRF2008 aligned	IGb08 aligned to ITRF2008	VTRF2014 aligned to ITRF2008
Datum definition	Minimum constraint	Minimum constraint	Free NEQ
Ellipsoid flattening	298.257810	298.25722 (WGS84)	298.25722 (WGS84)
Equatorial radius:	6378136.0 m	6378137.0 m (WGS84)	6378137.0 m (WGS84)
Solution	weekly	daily	session-wise
Time span	1993.0 ÷ 2015.0	1994.0 ÷ 2015.1	1979.0 ÷ 2015.0

All the ACs contributing to the reprocessing for ITRF2014 determination used the latest models and methods consistent with ITRF2014 guidelines.
For more details, see (http://ids-doris.org/combination/contribution-itrf2014.html; http://lUPus.gsfc.nasa.gov/IVS-AC_ITRF2013.htm and http://acc.igs.org/reprocess2.html).
For reader's convenience a snapshot of the IDS, IVS and IGS websites has been preserved as files in the supplementary material. IDS, IVS and IGS modeling standards are described respectively in Moreaux et al. (2016), Bachmann et al. (2016) and Rebischung et al. (2015).
In Figure 1 we have represented all the IDS sites included in the ITRF2014 combined solution, and co-locations with sites from other space geodetic techniques (SLR included).

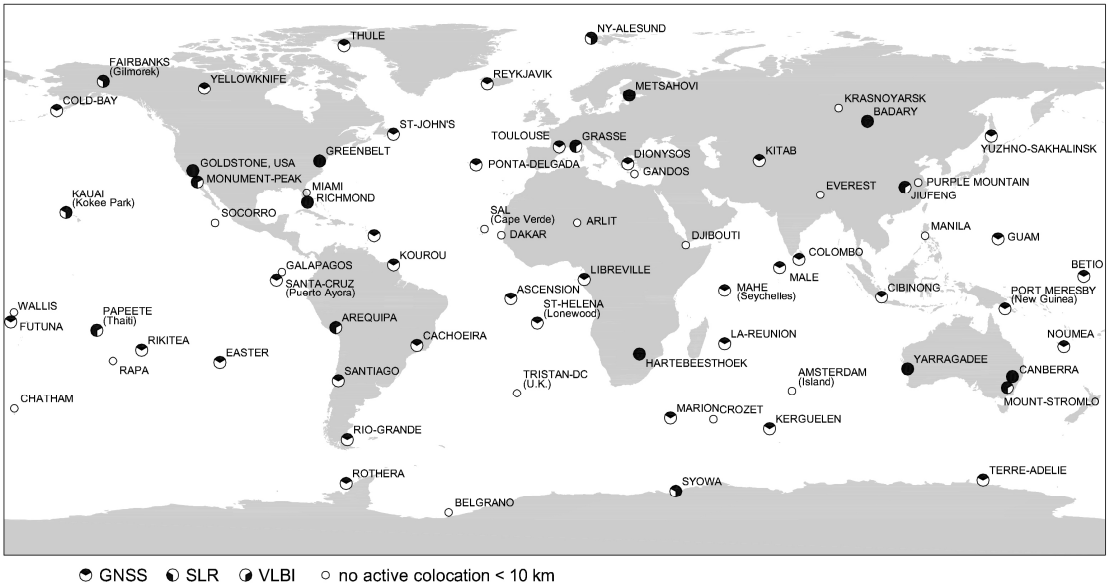

Figure 1: DORIS ITRF2014 network with indicated co-located VLBI, GNSS and SLR sites.

[1] Approximately half of these VLBI sites were occupied only a few times with mobile VLBI systems; several other VLBI stations are decommissioned or used for astronomic purposes and joined geodetic experiments a few times only.

The homogeneous global geographic distribution of the DORIS sites is clearly visible; we do not consider as co-located sites those having a distance larger than 10 km. For example, we have 35 DORIS-GNSS co-located sites. Among these sites, a total of 12 are co-located with VLBI. Only 8 sites have the SLR equipment and can be considered core sites, i.e., sites where all the four space geodetic techniques are available (or were available because some of them are no longer active).

One of the goals of this work concerns the evaluation of the quality of the underlying coordinate time series relative to each space geodetic technique contributing to ITRF2014. High quality is necessary to obtain high-accuracy multi-year solutions. This key task mainly consists of two steps. First, coordinate time series are analyzed to identify events, such as discontinuities and outliers. Second, this information is taken into account to model the accurate coordinate time series.

Estimated geodetic station coordinate time series include a long-term signal, discontinuities, data gaps, and cyclostationary stochastic processes, whose statistical properties vary periodically. They can be modeled by a functional and a stochastic model. The generally adopted functional model that combines a long-term linear trend, a step function, and cyclical components (Ostini, 2008) is not fully satisfactory. In particular, linear and multilinear models often appear to be inadequate to describe the long-term behavior of a site to obtain cyclostationary residuals.

To consider nonlinearity and to better describe the long-term signal that overcomes the inadequacy of multilinear models, we applied the method proposed by Roggero (2012), which treats the station motion as a discrete-time Markov process. We modeled the coordinate time series as a discrete-time linear system described by a finite state vector *x*, which evolves with known dynamics T through the epochs t (t ϵ [1, n]), has a system noise ν (with variance-covariance matrix Rνν), it follows that:

$$x_{t+1} = T_{t+1}x_t + v_{t+1}$$
$$y_{t+1} = H_{t+1}x_{t+1} + \epsilon_{t+1} \quad (1)$$

where y are the observed position P known with observation noise ϵ (with variance-covariance matrix $R\epsilon\epsilon$), and H is the partial derivative matrix that links the state vector x to the observations y. For a system with slow dynamics, e.g., coordinate time series, the motion can be approximated by a constant velocity model in T where the position p and the velocity $\dot{p}$ are the two elements of the state vector $x = [p, \dot{p}]$ with system noise $v = [v_p, v_{\dot{p}}]$.

For a discrete-time Markov process, the next state depends only on the current state and not on the preceding sequence of events. Kalman filtering plus smoothing has been used to update the information in the state space model. The estimated state vector $\hat{x}$ by Kalman filtering plus smoothing at different epochs has an optimal solution, which is equivalent to the least square approach, including the dynamics, as shown using simulated data by Albertella et al. (2005), and using real data by Tornatore & Cazzaniga (2009). The outliers are not rejected but properly weighted according to the system and observation noise in the estimation procedure.

We have to consider that the coordinate time series that we are studying on have been calculated in a different datum according to the single space geodetic technique. It's worth to note that in a network adjustment the coordinates and the variance covariance matrix are datum dependent, and only the estimated variance factor $\hat{\sigma}_0^2$ is datum independent. Therefore in our analysis we have to consider the datum definition of the compared solutions. While the IDS and the IGS submitted minimum constrained solutions, IVS submitted a free normal equations (NEQ) solution. In both cases the datum does not introduce distortions in the internal structure of the network. Minimum constraint network conditions are based on the assumption

that the reference frame of the estimated coordinates can be compared to an a priori reference frame, by a 7-parameter transformation. The time series of transformation parameters and station residuals can be analyzed in order to check the quality of the solution. This has been done by Bloßfeld et al. (2016) for IDS, by Rebischung et al. (2015) for IGS and by Seitz et al. (2015) for the four techniques realizing the DGFI2014 TRF. The same periodic effects in station coordinates residuals have been observed in the datum parameters and EOP time series.
Horizontal coordinates and velocities are highly correlated with datum rotations, while the vertical component is correlated with the scale factor, and all the three coordinates are correlated with the geocenter translation. Even if we are examining the station Up coordinate residuals, after removing the biases and a long term non-linear trend, they remain correlated with both the scale factor and the geocenter coordinates. Orbital effects can impact both the coordinates and the datum; for example GNSS orbits radial error can affect the scale factor, with a correlated impact on the estimated Up. DORIS and GPS draconitic harmonics have been detected both on station coordinates residuals and on datum parameters (Rebischung et al., 2015; Bloßfeld et al., 2016). Due to this correlation, the estimated amplitudes can be biased or scaled, while the frequency and the phase are datum invariant. For this reason amplitudes of residual signals that will be estimated during the harmonic analysis (see Section 5), separately for each technique, have to be treated carefully in the inter-technique comparison.

3. Model of discontinuities

Discontinuities may occur for a number of reasons, such as equipment changes, station movements, and changes in data processing strategies, data acquisition procedures and exceptional environmental conditions. All these effects must be identified precisely for reference frame realization. With advanced data analysis methods, discontinuities caused by some environmental phenomena in the signal can be detected in the coordinate time series based on the space geodetic techniques.
Lists of discontinuities of known origins (e.g., list of earthquakes or changes indicated in the station information files) are documented for all the space geodetic techniques, and these have been assumed a priori as candidate discontinuity epochs. However, discontinuities associated with any event of unknown reason also exist and need to be detected and removed, since stations that exhibit discontinuities would certainly produce biases in the estimated velocities (Altamimi et al., 2013), thus adding dedicated variables to the original state–space model of the time series. The second-order discontinuities (velocity change) were not considered because they were already taken into account in the long-term signal. The third-order discontinuities (harmonic signature change) were not added to the model because any change in the model during reprocessing of input time series for ITRF2014 was avoided (for example, different conventions, new loading, or tidal models were not introduced).
Discontinuity detection methods are critical for time series analysis. We have modeled time series according to the approach indicated in Section 2. To take into account estimation of discontinuities we have modified the model described in Equation (1) as follows:

$$\begin{aligned} x_{t+1} &= T_{t+1}x_t + B_{t+1}b_t + v_{t+1} \\ y_{t+1} &= H_{t+1}x_{t+1} + C_{t+1}b_t + \epsilon_{t+1} \\ b_{t+1} &= b_t \end{aligned} \tag{2}$$

where the bias vector b is constant with steps, and it is connected to the dynamics of the system by matrix B, whose elements are assumed to be equal to zero if the bias only affects the

observed position; vector b is linked to the observations through matrix C, whose elements can have value 0 or 1 and represent the occurrence of the biases in the time series. The size of matrices B and C is determined by the number of observation epochs and unknown number of gaps to be estimated. If some documented discontinuities exist, then matrices B and C are a priori known, and we use the lists of known discontinuities provided by each International Service. The adequacy of the estimated discontinuity model was tested by using the variable ratio, such as that in the case of normal residuals with a χ^2 distribution in (Roggero, 2012).
To demonstrate an example of the Up component time series and discontinuity estimation, we present the time series estimated for the DORIS site of Metsahovi. The currently running station is called MEUB, the previous ones were called META and METB. The time series exhibit heteroskedasticity, i.e., a variable standard deviation (σ) of the Up component over time. This is clearly shown in Figure 2(a) by a gray scale color bar. Generally, σ decreases with time because of improvements in the observing technique and the processing algorithms. Two significant discontinuities of +8 and -9 mm in the correspondence of the changes of the beacons at the site were detected and are also clearly visible in Figure 2(a).
A mean velocity of 3.66±2.28 mm/year was estimated over the entire data set as the mean value of parameter $\dot{p}$ (estimated at each epoch). The properties of the residuals after the removal of the discontinuities and long-term model, presented in Figure 2(b), are almost cyclostationary with the exception of their heteroskedasticity.

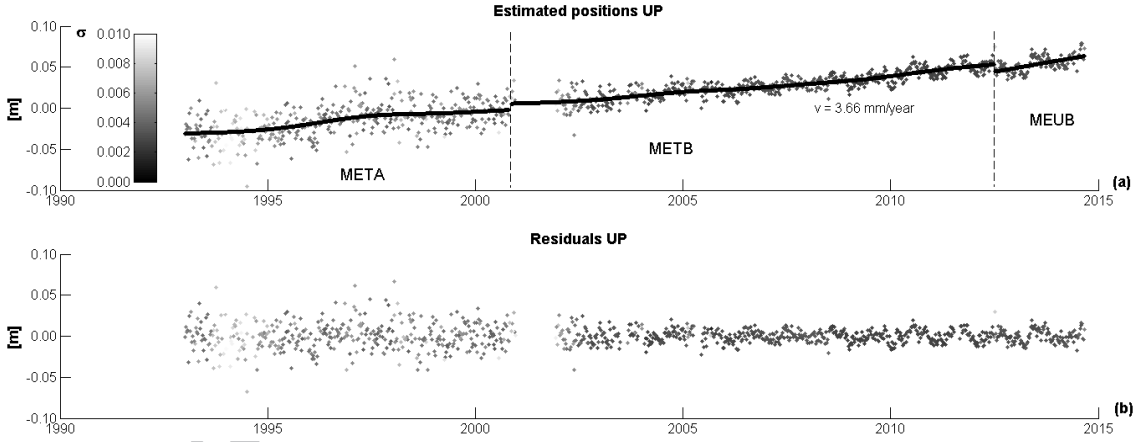

Figure 2: Metsahovi DORIS site Up time series with jumps in correspondence with beacon changes (a) and residuals (b) almost cyclostationary. The grayscale color bar represents σ of the Up component, which is higher in the first years of observations.

For each space geodetic technique, the following discontinuities are documented: 63 for 71 IDS sites (54% of seismic origin), 33 for 159 IVS sites (59% of seismic origin), and 652 for 1845 GNSS sites (17% of seismic origin). These numbers are not directly comparable among them and with those presented e.g. by Seitz et al. (2015). This happens for several reasons at first, our percentages are based on the number of sites of the different IDS, IVS and IGS networks and not on the number of stations (we first concatenated different time series of stations related to the same sites). Then, the criteria related to single techniques differ because of concerns with regard to whether an earthquake should be counted or not: IVS ACs report a discontinuity only if the earthquake affected the time series of the site coordinates, whereas IDS considers only the earthquakes with magnitude larger than 6 in the vicinity of DORIS sites (less than 500 km) based on USGS(United States Geological Survey) earthquake event notifications, while IGS considers as a possible source of discontinuities all the earthquakes. Sever-

al documented discontinuities are attributed to hardware changes in the antenna and/or receiver, hardware repairs, or relocation of stations.

4. Modeling long-term signals

Linear trends, nonlinear and non-periodic signals, and periodic signals with a period longer than the time series length are included in the model of long-term signals. Thus, the linear trend is only one component of the long-term signal. However, to obtain cyclostationary model residuals, nonlinear long-term signals must be taken into account. According to the time series model based on the state space approach, as described in Equations (1) and (2), the model can follow different dynamics by setting different values for the system noise variance $\sigma_v^2 = \left[\sigma_{v_p}^2, \sigma_{v_{\dot{p}}}^2\right]$.

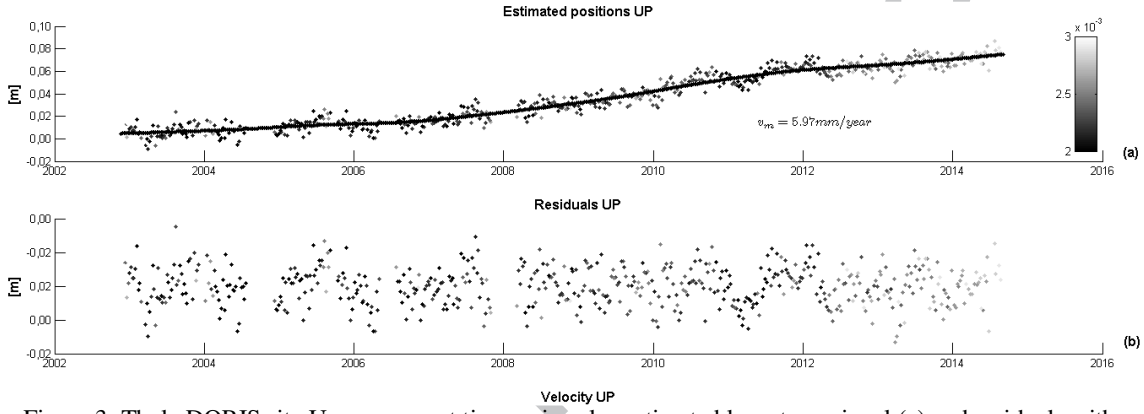

Figure 3: Thule DORIS site Up component time series plus estimated long-term signal (a) and residuals with quasi-cyclostationary behavior (b). A mean velocity v_m = 5.97 mm/yr has been estimated as a mean value of $\dot{p}$.

The choice of the system noise variance is critical, and it does not depend on the observing technique but only on the system dynamics. The standard deviation of the system noise $\nu = \left[\nu_p, \nu_{\dot{p}}\right]$ was fixed empirically as in Roggero (2016), assuming $\sigma_{\nu_p} = 10^{-6}$ m and $\sigma_{\nu_{\dot{p}}} = 10^{-6}$ m/yr for all the techniques. As described in Equation (1), the system noise represents the variability of the state vector $x = [p, \dot{p}]$ from an observation epoch to the subsequent one. It has not be confused with the much more larger observation noise ϵ, whose variances σ_P^2 are the diagonal elements of the observation variance-covariance matrix $R\epsilon\epsilon$, that are known from the respective intra-technique solutions. Figure 3 shows the long-term signal of the Up coordinate time series of the Thule DORIS station THUB. Velocity $\dot{p}$ is estimated at each epoch of the state vector, whereas the mean value of velocity v_m = 5.97±2.98 mm/yr was computed as the mean value of the instantaneous velocities $\dot{p}$. The moderately large value of the mean velocity standard deviation σ_{v_m} can be due to the variability of $\dot{p}$ that ranges in the interval 2-12 mm/yr.

5. Harmonic analysis

The FAMOUS software, used at this step to perform the harmonic analysis of residual time series, was explicitly developed to detect sets of frequencies in discrete and unevenly sampled data sets. As we have explained in Section 2, our set of coordinate residual time series obtained from IDS, IVS and IGS are unevenly sampled. In literature (see Section 1 for references), the spectral analysis of such data is generally carried out by using a Lomb periodogram or comparable methods. However an interpretation of these periodograms can be

ambiguous because artificial spikes can appear due to the irregular observing window that contributes to the real spectral content.

The approach used by the FAMOUS algorithm identifies the most powerful spectral line by estimating periodograms with a least squares adjustment. The next most significant spectral line is searched for calculating periodograms in the residual data set after removing the first detected spectral line. Nonlinear optimization adjustment is carried out at each step to improve frequency location and trend estimation. Signal-to-noise ratio (SNR) test is conducted only on the most significant spectral lines.

The heterogeneity of the height residual time series was considered by adding a feature to the FAMOUS algorithm to obtain more reliable estimates of spectral lines. In particular, the least squares adjustment of periodograms and nonlinear optimization were weighted by using the inverse of the square of the site formal error in the height time series.

The harmonic analysis applied by FAMOUS has some advantages over other approaches, such as fast Fourier transformation, using basic sine and cosine functions in the decomposition process to generate a frequency spectrum. FAMOUS decomposes a time series *y(t)* as follows:

$$\psi(t) = c_0 + \sum_{i=1}^{k} c_i \cos(2\pi\nu_i t) + s_i \sin(2\pi\nu_i t) \tag{3}$$

where k is the maximum number of searched frequencies, whereas c_i and s_i are polynomials of time expressed as

$$\begin{aligned} c_i &= a_i^0 + a_i^1 t + a_i^2 t^2 + \cdots + a_i^p t^p \\ s_i &= b_i^0 + b_i^1 t + b_i^2 t^2 + \cdots + b_i^p t^p \end{aligned} \tag{4}$$

The polynomial degree $p = p(i)$ is automatically selected by FAMOUS for each frequency ν_i. The algorithm estimates the parameters (a_i, b_i, ν_i) using the model

$$min|y(t) - \psi(t)|^2 \tag{5}$$

which is a nonlinear least square that is sensitive to the starting values and solved in two steps by singular value decomposition and Levenberg–Marquardt minimization. The solution is also given in terms of frequency ν_i, amplitude A_i, and phase ϕ_i by $A \cdot cos(\omega t + \phi)$, and the signal can be reconstructed as

$$\psi(t) = c_0 + \sum_{i=1}^{k} A_i \cos(2\pi\nu_i t + \phi_i) \tag{6}$$

The decomposition of a time series by the classical Fourier methods requires stationary long-term series with constant sampling rate, equally weighted data values, and no gaps. FAMOUS can overcome these limitations by handling unevenly spaced time series. Tests of statistically significant spectral peaks are implemented with respect to SNR.

We employed the FAMOUS software to map the spectral content of the position residual time series with detections restricted to spectral lines with an SNR greater than three. This value was chosen because it was the first that allowed clear signal detection. In fact, the signals identified by using a lower SNR value are still unclear. In the following subsections, the detected frequencies above SNR = 3 are summarized separately for each space technique.

The overall detected signals can be categorized in three classes related to seasonal, draconitic (related to satellite orbit configuration), and tidal effects. The percentage of incidence for each class of signals is shown in square brackets, i.e., the number of sites where those frequencies of the signal are detected over the total number of sites.
From the point of view of data availability and distribution, the IGS coordinate time series are generally given in a single file for each site, with the exception of a few sites where two or more GPS receivers are co-located or connected to the same antenna. The IDS coordinate time series given in separated files for each DOMES number at the same observing site and a new DOMEs number is established at the same observing site when the hardware is updated. The IVS coordinate time series are generally given in a single file for each site, with the exception of sites where co-located VLBI static antennas exist or in the case of mobile antennas.

5.1. DORIS harmonic analysis

The DORIS-reprocessed time series for ITRF2014 calculation is called IDS02, its time span is from 1993.0 to 2015.0 and they are constituted by weekly solutions, unless some sporadic episodes of no acquisition introduces data gaps in the time series. The single station files need to be concatenated to obtain a complete time series of the site, while the epochs START and END of a station are assumed as discontinuities of the first order (position discontinuity). Seismic events near the DORIS sites have been reported since 1993 at (http://ids-doris.org/system/earthquakes-close-to-doris-sites.html), although not all of them affect the time series in terms of coordinate changes. A complete statistic on the DORIS sites was carried out using the station events available at (http://ids-doris.org/system/doris-stations-events.html), which starts with the Marion Island setup at 1/1/1980. In 71 sites, IDS reported 82 discontinuities in a time span of 35 years (1980.0–2015.0), whereas 63 a priori discontinuities in the interval (1993.0–2014.67) were assumed in the IDS02 (ITRF2014) cumulative solution. The discontinuities of seismic origin are 34 (54%), where 11 are attributed to beacon origin change (17%) and 18 are of unknown origin (29%). The oldest DORIS sites are Badary, that started in 1991/11/12 and Marion Island in 1987/05/15. However data before 1993.0 were not considered in the IDS02 solution and the mean length of the time series is approximately 17 years.
The harmonic analysis was carried out on the residuals of the time series of the Up component after discontinuity estimation and removal and de-trending of the long-term signal. The detected signal incidences in Figure 4 are computed as the number of sites where each signal is detected over the total number of sites [%]. In Figure 4, the signals denoted by dashed lines are the annual term and its harmonics (seasonal term), whereas those with continuous lines are the tidal harmonics. Table 2 indicates the expected and detected harmonic frequencies in cycle per year (cpy), and their periods in days and amplitudes are given in mm. The incidence of the detected signals was also reported in [%]. In the current paper, this incidence refers to the number of sites where signals with period P (in the interval $P\pm\sigma$) were detected. For example, the annual term was detected in 15% of the sites in a period between 353 and 373 days (363±10).

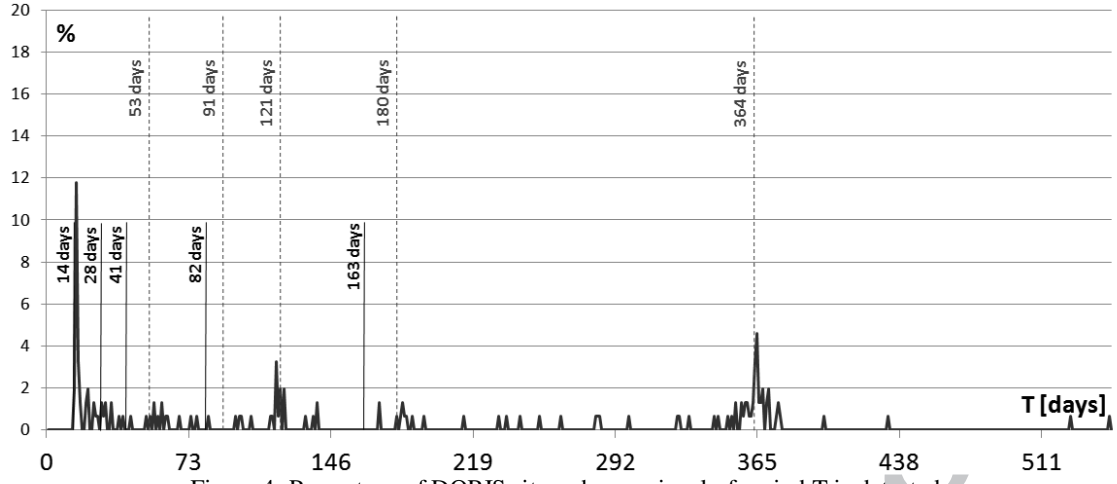

Figure 4: Percentage of DORIS sites where a signal of period T is detected.
(The periods of the expected tidal (——) and solar (– – –) harmonics are evidenced)

Table 2: Detected signal period and amplitude for DORIS sites.
(The values inside the square brackets are the percentages of incidence)

	DORIS harmonics [days]				**mean amplitudes [mm]**	
	expected		**estimated**			
cpy	**solar**	**tidal**	**solar**	**tidal**	**solar**	**tidal**
1	365.3		363±10		10.3 [15.0%]	
2	182.6		183±3		8.8 [3.9%]	
3	121.8		118±3		7.5 [9.2%]	
26.74		13.6		15±1		6.1 [18.3%]

Three solar year harmonics were detected (first, second, and third) plus another significant signal with a period of 15±1 days. Although we are close to the minimum sampling period of 14 days (Nyquist period) for the weekly time series, the solar harmonics had a strong signal, which was clearly detected in 18.3% of the DORIS stations. The same signal was more precisely detected in the IVS and IGS time series. Thus, we classified this signal as a tidal signal. However, its origin is still unclear. The annual and semiannual tidal effects cannot be distinguished by other seasonal effects because of their seasonality. Observing DORIS draconitic signals is difficult. In fact, even if artifact signals at the yearly nodal period for SPOT, at the 117.83 days draconitic period for TOPEX/Poseidon and at the 117.32 days draconitic period for Jason satellites are known (Willis et al., 2012), they could be aliased in the first and third solar harmonics with period of 365.3 and 121.8 days. However, we cannot exclude the draconitic origin of the detected signal with a period of 118±3 days.

Bloßfeld et al. (2016) in their analysis of the weekly 7-parameter similarity transformations (IDS-only epoch reference frames) w.r.t. the combined IDS02 and DTRF2008 (IDS-only) solutions, detect in the scale parameter significant peaks at 14.7 days (only in the IDS02 submission) and 22.36 days (only in the DTRF2008 solution). A significant peak at about 58 days (≈117/2) has been also detected by the same authors and likely corresponds to a Jason or TOPEX/Poseidon semi draconitic harmonic. Our results on coordinates time series cannot be directly compared to the analysis from Bloßfeld et al. (2016) that relates to the weekly IDS

reference frame transformation parameters. However the scale factor harmonic analysis can be quite reasonably compared to the harmonic analysis of the Up coordinates time series.

5.2. VLBI harmonic analysis

The IVS Up component time series analyzed in this work is derived from the combined solution calculated for ITRF2014. This combined solution is named ivs2014a. It spans from 1979.0 to 2015.0 and includes 159 radio telescopes (including mobile, fixed, and decommissioned radio telescopes). The VLBI network of an observing session can have a minimum of three radio telescopes to a maximum of 20 (only one experiment with 32 sites was carried out in 2009, and another experiment with 21 sites was conducted in 2013). One session consists of a set of observations that are carried out during a 24-h interval. However the outliers handling and elimination, applied differently by the individual ACs, can shift the middle epoch of the session.

The first problem in harmonic analysis was the choice of the sites that fulfilled the requirements because of the extremely uneven sampling of the IVS time series data set. Nevertheless they can be analyzed with the FAMOUS software that should also be able to analyze data with even sampling. This analysis failed in several cases, or no statistically significant signals were found. These problems occurred for the IVS time series with an observation history shorter than 5 years. In addition to the data span, we had to consider another parameter: the frequency of the sessions. This new parameter varies from a few sessions per year up to two sessions per week, with the exception of the Greenbank, a 85-foot radio telescope (USA) that carries out a mean of five sessions per week and of seldom daily experiments carried for a fixed periods and for dedicated networks of stations. The criteria used to choose the IVS sites for analysis were those with at least 5 years of observations and at least 2 sessions per month; only 25 sites fulfill these criteria. For these sites, eight discontinuities in the Up direction were detected and removed.

In Figure 5, we can observe two classes of signals related to seasonal (represented with dashed lines) and tidal effects (continuous lines). The expected and estimated harmonic frequencies, periods, and amplitudes along with their percentages of incidence are reported in Table 3.

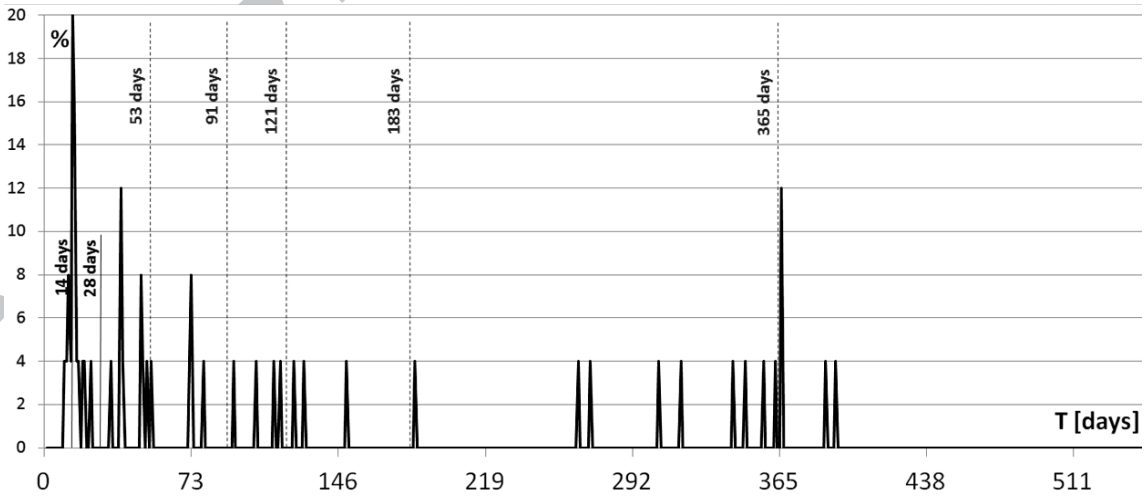

Figure 5: Percentage of VLBI sites where a signal of period T is detected.
(The periods of the expected tidal (——) and solar (– – –) harmonics are evidenced)

Table 3: Detected signal period and amplitude for VLBI sites.
(The values inside square brackets are the percentages of incidence)

	VLBI harmonics [days]					mean amplitudes [mm]		
	expected		estimated					
cpy	solar	tidal	solar	tidal	unknown	solar	tidal	unknown
1	365.3		366±1			3.5 [12.0%]		
9.61					38±1			5.4 [16.0%]
24.73		14.8		14±1			3.0 [20.0%]	
26.74		13.6		12±1			2.4 [16.0%]	

The annual signal was detected for 12% of the analyzed sites with a mean amplitude of 3.4 mm, which was lower than the amplitude observed in the IDS time series and is more coherent with IGS data (see Table 4). Among the 25 IVS sites analyzed in this work, 11 have a time series sampling higher than a week, thereby enabling the detection of some short wavelength signals. In particular, at a period of approximately 14 days, we observed two different signals at 12±1 and 14±1 days. The signal with period of 14±1 days affects 5 stations: Hobart 26 m, Matera, Westford, Ny-Ålesund and Wettzell, while the signal with period of 12±1 days affects 4 stations: Hobart 26 m, Matera, Ny-Ålesund and Wettzell. The larger amplitudes are in Hobart (respectively 5.5 and 4.8 mm), while in the other stations we observe amplitudes between 1.0÷2.5 mm. These signals can be compared with the lunisolar fortnightly cycle *Mf* with duration of 13.66 days and the lunisolar synodic fortnightly *Msf* with a duration of 14.76 days (Doodson, 1921). Another signal of unknown origin was detected at a period of 38±1 days with 16% incidence.

5.3. GNSS harmonic analysis

The global IGS network is densely distributed even if a higher number of sites are placed in the northern hemisphere. It is made up of 1845 sites whose data span is 1993 to the present. GNSS time series consist of daily solutions of 24 h. Thus, the spacing among data is almost regular. Reprocessing of IGS global tracking network back to 1994 contributing to ITRF2014 was carried out under the project called REPRO2, which produced daily and weekly solutions. The details on the reprocessing, performed using the latest available models and methodology, are reported at (http://acc.igs.org/reprocess2.html), whereas the daily and weekly SINEX are available at (ftp://igs-rf.ensg.eu/pub/repro2). To be coherent with the minimum time span of the IDS and the IVS data harmonic analysis, also for the IGS time series, we rejected the sites with less than 5 years of data, thereby reducing the total number of sites to 1252. Note that Blewitt & Lavallée (2002) recommend a minimum time span of 2.5 years, but as explained in Section 5.2, the FAMOUS analysis failed in several cases, or no statistically significant signals were found, using the IVS time series shorter than 5 years. The documented discontinuities are distributed in the soln_IGb08.snx file for the analyzed sites. Among a total of 416 documented discontinuities, 300 were marked as statistically significant, estimated, and removed (72% of the total). For daily time series, the highest frequency is 182.5 cpy, which is equivalent to a period of two days. We also identified the significant signals with a sub-daily accuracy. Figure 6 shows the percentage of incidence of the detected signals, highlighting the solar year harmonics (seasonal term) with dashed lines, the draconitic harmonics with continuous lines, and the tidal harmonics with dotted lines.

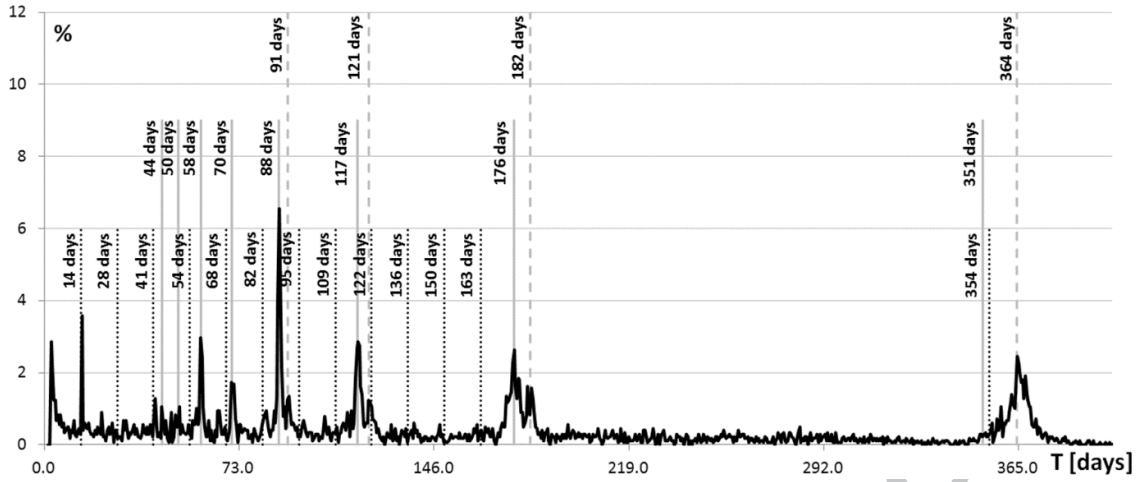

Figure 6: Percentage of GNSS sites where a signal of period T is detected.
(The periods of the expected draconitic (——), solar (– – –) and tidal (·····) harmonics are evidenced)

Table 4: Detected signal period and amplitude for GNSS sites.
(The values inside square brackets are the percentages of incidence)

GNSS harmonics									**mean amplitudes [mm]**		
expected						**estimated**					
solar		**draconitic**		**tidal**		**solar**	**draconitic**	**tidal**	**solar**	**draconitic**	**tidal**
[cpy]	**[days]**	**[cpdy]**	**[days]**	**[c]**	**[days]**	**[days]**			**A [incidence%]**		
1	365.3	1	351.2	26	354.1	364.4±4.0	351.5±3.0	355.0±3.5	4.8 [35.4%]	3.8 [5.0%]	3.1 [3.6%]
2	182.6	2	175.6	12	163.4	182.4±2.0	175.8±1.8		2.6 [10.8%]	1.8 [20.3%]	
3	121.8	3	117.1	9	122.6	121.4±0.4	117.6±1.6		2.8 [7.8%]	2.2 [15.3%]	
4	91.3	4	87.8	6	81.7	91.0±0.4	87.8±0.8	81.6±0.2	1.5 [5.2%]	1.7 [17.9%]	1.6 [5.2%]
		5	70.2				70.0±0.6			1.2 [6.8%]	
		6	58.5				58.4±0.4			1.2 [8.2%]	
		7	50.2				50.4±0.2			1.4 [3.4%]	
		8	43.9	3	40.9		44.0±0.2	40.9±0.1		1.1 [2.6%]	1.1 [3.2%]
				1	13.6			13.7±0.1			1.7 [5.7%]

The power spectra of the GNSS coordinate time series are widely studied since the observations are frequent and quite uniform in time and space. Analysis of spatial correlation of the detected signals can be difficult for some geographic areas with a poorer coverage. Blewitt and Lavallée (2002) and other works, such as that of Collilieux et al. (2007) and Gazeaux et al. (2013), analyzed the spectral content of GNSS height time series and clearly detected annual and semi-annual signals, as well as higher harmonics. Roggero (2016) analyzed the REPRO1 weekly time series by using the same methodology adopted in the present work, detecting most of the signals reported in Table 4 despite the lower accuracy and resolution.

In Table 4, the frequencies are reported in cpy for the solar harmonics, cycle per draconitic year (cpdy) for the draconitic harmonics, and in cycles (c) of the lunisolar fortnightly period *Mf* for the tidal harmonics. As expected, the detection accuracy is at the sub-daily level and reaches 0.1 days at the higher frequencies. The solar harmonics are evident up to the fourth harmonic (4 cpy) with a high incidence for the annual and semi-annual term, which can also include the solar annual and solar semi-annual tidal effects. Figure 6 indicates that the solar harmonic peaks are generally aliased by other signals with a fundamental frequency of 1.04±0.01 cpy. The peaks can have two different origins in the GNSS time series, as discussed in Ray et al. (2008). The fundamental frequency at 1.04 cpy (351.2 days) corresponds

to the GNSS draconitic year, the period at which the GPS constellation orientation with respect to the Sun repeats. The fundamental tidal frequency is the lunisolar fortnightly period of 13.66 days (*Mf*), having a clearly visible effect also at the 3rd, 6th and 26th harmonics. The tidal 26th harmonic, with period of 1.03 cpy (354.1 days), and the draconitic year, with period 351.2 days, have been detected even if aliased by the solar annual term. The draconitic harmonics were detected up to the eighth harmonic, whereas the tidal terms were observed only for some frequencies.

The detected signals are reported in Table 4 and grouped in the same line in different terms, namely, solar, draconitic, and tidal, which can be mutually aliasing. For example, the third line of the table shows the third solar harmonic, the third draconitic harmonic, and the 9 *Mf* tidal harmonic with a period of 121.8, 117.1, and 122.6 days, respectively. Practically, distinguishing the two signals at 121.8 and 122.6 days while the peak is at 117.1 days is not possible, as shown in Figure 6. In this case, as for the annual and semi-annual term, the tidal effect must be considered as contributing to the seasonal term. The lunisolar fortnightly cycle of 13.66 days has also been detected, but has a lower incidence (5.7%) with respect to the IDS and the IVS time series. The other two peaks at 40.9±0.1 and 81.6±0.2 days are coincident with three and six *Mf* cycles. Some non-explained peaks at 97, 105, 138, and 148 days are close to 7, 8, 10, and 11 *Mf* cycles (95, 109, 136, and 150 days) but non-coincidental. These signals need further investigations to determine other tidal effects on the IGS time series. Our model, which considers tides with multiple wavelengths of *Mf*, is a simplification of the actual phenomena.

6. Discussion of the results for DORIS, VLBI, and GNSS at co-located sites

Generally, to achieve and maintain the ITRF, we do not only need the observations from the networks of the four space geodetic techniques (DORIS, VLBI, GNSS, and SLR) but also the local ties, i.e., measured vectors at co-located sites, that employ at least two of these techniques to connect the different reference points of the instruments used by each technique. To achieve the goals of the Global Geodetic Observing System (GGOS), a reference that will allow position accuracy in mm and stability over decades of 0.1 mm/year was established by the GGOS Bureau of Networks and Observations to create a homogeneous network covering the entire Earth with 32 new technology core sites co-located with DORIS, VLBI, GNSS, and SLR equipment (Pearlman, 2015). Large investments and efforts are requested in this direction for coming years. Indeed, as demonstrated in Figure 1, currently only eight sites all over the world have all the four co-located space geodetic techniques.

For all the 12 co-located sites where the three techniques studied in this work: DORIS, VLBI, and GNSS are available, we report the velocities estimated by using the procedure described in Section 2. However, as already noted about the datum definition, coordinates and velocities are datum dependent. Even if all the used datums are aligned to the ITRF2008, they can be biased and this inter-technique comparison must be verified in future using the output ITRF2014 coordinate time series.

Despite these cautions, it is possible to draw some preliminary indications from the velocities estimates shown in Table 5. These values were estimated over the entire reprocessed time series for ITRF2014 as the mean value of the parameter $\dot{p}$, estimated at each epoch together with the parameter p, see Section 2. The STD was computed with respect to the mean station velocity $\bar{v} = (v_{IVS} + v_{IDS} + v_{IGS})/3$. The low velocity STD indicates good coherence between the techniques, but a more detailed analysis outlines specific problems that have not yet been solved in the inter-technique comparison: incoherent data time span and non-uniform time series length, data sampling and handling of discontinuities due to hardware change.

The more uncertain case for the Up velocity coherence is the Yarragadee station in Australia, where the 12 m VLBI antenna provides a different velocity with respect to GPS and DORIS results, which are coherent between them. The poor consistency of the IVS data can be attributed to the different time spans of the three time series for this site: IDS spans from 1993.0 to 2014.7 (a 21.7-year duration), IGS spans from 1998.8 to 2015.1 (a 16.3-year duration), and IVS spans from 2011.4 to 2015.0 (a 3.6-year duration). This result confirms the criteria used in Section 5.2 to select a VLBI station to apply harmonic analysis: at least 5 years of observations and at least 2 sessions per month. Moreover, the IVS data before 2013.5 are sparse and noisy with a mean sample interval of 10 days and a mean Up STD of 5.6 mm, whereas after 2013.5 we have data with a mean sample interval of three days and a mean Up STD of 1.8 mm. In the second interval the estimated velocity of the Up component is 2.1 mm/year compared with the 3.5 mm/year obtained from the entire data set, also the coherency with respect to IDS and IGS velocities is slightly better. However, after 2014, when the number of sessions of the AUSTRAL observing program increased significantly, the IVS time series appeared to stabilize, but the time span is excessively short to obtain a reliable estimate of the velocity.

Other three sites, Canberra, Fairbanks and Syowa, show velocity STDs larger than 2 mm/year in the horizontal components. The quite large STD in Canberra and Syowa is partly due to the poor data availability of the time series, but there are also other reasons. Canberra North velocity has a STD of 2.8 mm/year, the DORIS velocity for the Orroral site is 24.4 mm/year and it is not coherent with the VLBI (18.9 mm/year Tidbinbilla site) and the GPS (18.1 mm/year) estimates. The Orroral site (co-locating DORIS and SLR now obsolete) is about 27 km south of the Tidbinbilla site (VLBI and GPS); even if the VLBI station has only 12 observation sessions in the long observation interval between 1982 and 2015, VLBI and GPS estimates are very similar. The difference with the DORIS estimate can also be explained considering the limited time span of the DORIS observations, in the intervals 1993.0-1996.3 (station marker ORRA) and 1997.0-1998.8 (station marker ORRB). Moreover, Orroral site was occupied very early in the DORIS history: it was before that major upgrades in the monumentation, augmentation of the DORIS LEO satellite constellation and data processing improvements were implemented (Valette et al., 2010; Bloßfeld et al., 2016). Mt. Stromlo observatory is actually closer to Tidbinbilla, even if the VLBI and SLR/GNSS/ DORIS are on opposite sides of a mountain.

The VLBI station in Syowa has only 66 sessions between 2000 and 2015 with a mean of about 4 sessions per year, the VLBI estimate of the East component is poorly coherent with DORIS and GPS estimates, the inter-technique STD of 2.2 mm/year.

Fairbanks (Gilmore Creek) DORIS has quite noisy data and a strong annual signal before 2000. Yaya and Tourain (2010), see Figures 11 and 12 of the paper, identified seasonal multipath phenomena, due to the presence of trees and reflection on ground, affecting the DORIS data. These effects along with the Denali Fault earthquake may have degraded the quality of the DORIS solutions and the agreement with the other techniques. Fairbanks station in Alaska is 150 km North of the Denali Fault Earthquake (Oct 23, 2002) when the GPS station shows a seismic discontinuity of +17 mm in the Up component; then the station coordinates time series show a 2 years long post seismic transient.

Some stations show a good inter-technique agreement, even if the estimated velocities must be compared carefully for different reasons. In Goldstone, GNSS and VLBI sites have same

distance from the DORIS site. DORIS is near to the "Venus site" (DSS 13), whereas the GNSS is some km away near the 70 m DSS 14 site. The Richmond geodetic site was destroyed during the passage of hurricane Andrew, in August 1992, but the ITRF2014 reprocessing involves only the data back to 1993. Data from the three techniques are contemporary available only during some limited intervals. GNSS station RIC1 has continuous observations from 1997 to 2000, while they are carried out episodically after 2000. DORIS RIDA station observed from 1993 to 2005 and has a wide data gap in 2002. VLBI observed only from 1984 to 1993 when it was terminated by the host agency. In Greenbelt, Maryland, we have completed GNSS time series from 1993 up to 2015, whereas VLBI has very few observations from 1993 to 2008 and a DORIS station was established only in 2000 and is still operating. Greenbelt site has also very different time intervals of data availability from the three techniques, but in this case this has apparently no consequences on the agreement between the estimate velocities. The reason can rely on a quite stable velocity for this site, with small variations in the 1993-2015 intervals.

Table 5: The estimated component velocities and mean STD [mm/year] for the 12 DORIS/VLBI/GNSS co-located sites. The GNSS velocities in Richmond and Canberra refer to RCM6 and TID2, respectively.

	Velocity E [mm/year]				**Velocity N [mm/year]**				**Velocity Up [mm/year]**			
Station	**VLBI**	**DORIS**	**GPS**	**STD**	**VLBI**	**DORIS**	**GPS**	**STD**	**VLBI**	**DORIS**	**GPS**	**STD**
Badary	6.4	6.4	7.0	**0.3**	27.0	26.0	27.6	**0.7**	1.5	1.3	-0.1	**0.7**
Canberra (Orroral/Tidbinbilla)	55.4	54.3	55.3	**0.5**	18.9	24.4	18.1	**2.8**	-1.1	-2.0	-1.2	**0.4**
Fairbanks (Gilmore Creek)	-23.9	-30.4	-29.8	**2.9**	-7.5	-4.5	-9.4	**2.0**	3.5	3.7	1.4	**1.0**
Goldstone (Mojave)	2.1	2.9	3.4	**0.5**	-16.9	-19.6	-18.4	**1.1**	0.8	0.0	-1.4	**0.9**
Greenbelt	-1.2	-2.9	-3.6	**1.0**	-15.7	-14.2	-14.4	**0.7**	-1.0	-1.9	-1.0	**0.4**
Hartebeesthoek	18.1	18.8	20.5	**1.0**	17.4	18.3	16.9	**0.6**	0.1	-0.7	0.3	**0.4**
Kauai (Kokee Park)	-36.2	-34.6	-35.3	**0.7**	-62.1	-62.1	-62.5	**0.2**	0.9	0.1	2.0	**0.8**
Metsahovi	-12.9	-12.1	-13.0	**0.4**	19.5	20.3	19.3	**0.4**	2.9	3.7	3.6	**0.4**
Ny-Ålesund	14.2	13.9	14.3	**0.2**	10.3	9.3	10.2	**0.4**	7.4	6.1	7.4	**0.6**
Richmond	-4.3	-2.1	-1.7	**1.1**	-9.7	-10.8	-10.5	**0.5**	0.1	0.1	0.2	**0.0**
Syowa 11-m	4.0	-1.2	2.8	**2.2**	-3.4	-3.0	-3.9	**0.4**	-1.0	0.1	1.0	**0.8**
Yarragadee 12m	60.8	57.4	58.0	**1.5**	40.7	39.2	38.9	**0.8**	3.5	-0.8	-0.6	**2.0**

Among the 12 co-located stations (DORIS, VLBI, and GNSS), we show a more detailed analysis of the Ny-Ålesund site, Svalbard Islands, that has moderately long time series (about 20 years) for all the 3 techniques. We obtained consistent results in the detected signals, frequency, amplitude, and phase for all the 3 techniques, unlike previous studies (Kierulf et al., 2009) that show inconsistent results among different observing techniques. Using the time series modeling described in Section 3, after discontinuities detection, estimation and removal in the Up component, we calculated the mean velocities in the time interval of data acquisition for each new marker monumented for each technique. We report these values in Table 6 compared to the ITRF2008 and the ITRF2014 uplift velocities.

Concatenation of the Up time series for IDS stations SPIA (till 30/6/1999), SPIB (29/07/1999-15/08/2003) and SPJB (after 19/09/2003) together with IVS NYLES20, and IGS NYAL station are shown in Figure 7. Superimposed to the concatenated time series there are respectively IDS, IVS and GNSS estimated long-term models (continuous gray line) and the estimated

discontinuities (black bullets). The unit measurement for the Up component, discontinuities, coordinate standard deviations and the residuals are in meters.

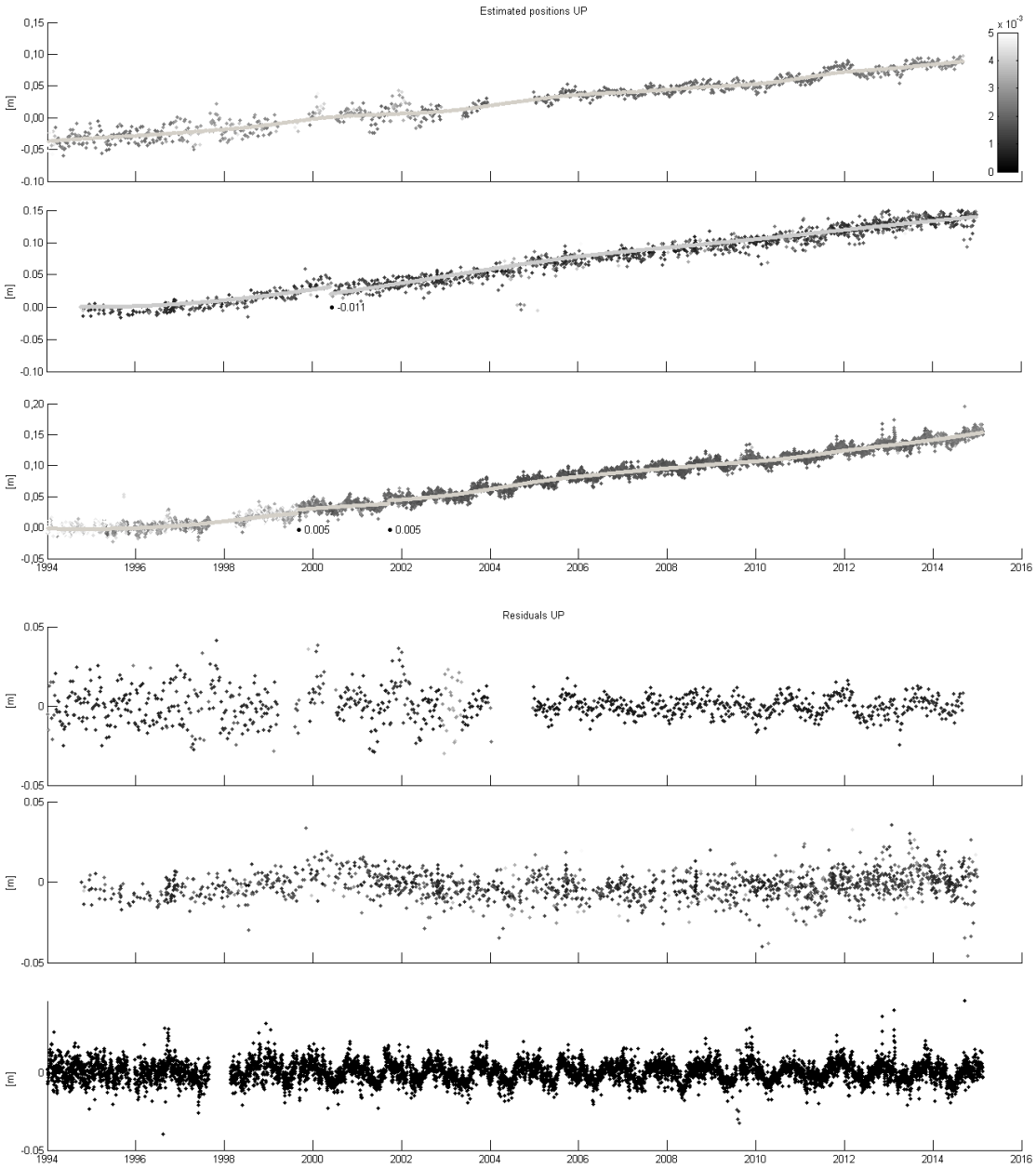

Figure 7: Ny-Ålesund IDS, IVS and IGS concatenated Up component time series and quasi-cyclostationary residuals with respect to the long-term model.

By comparing the three time series, we can see that IDS and IGS exhibit more evident periodic signals and heteroskedasticity as data precision increases with time. In IDS, we have more noisy and sparse data with fairly important data gaps that may even be longer than one year. In the IVS time series we have detected and estimated an un-documented jumps of -11 mm in 2000.4, the reason of this bias is still unclear.

Table 6: Geodetic stations in Ny-Ålesund, time spans and vertical velocities. The estimated values of Table 5 and the directly comparable ITRF2008 and ITRF2014 values are in bold. A velocity discontinuity has been assumed in ITRF2014 for NYAL in 1998:091 and SPIB in 2002:075.

Service	Dome n.°	Marker	Start	End	V_{UP} [mm/yr]		
					ITRF2008	ITRF2014	Estimated
IGS	10317M001	NYAL	1994:002	1998:091		3.40	2.14
	10317M001	NYAL	1998:092	2015:045	8.40	7.67	8.22
	10317M001	NYAL	1994:002	2015:045		-	7.39
	10317M003	NYA1	1998:070	2015:045	**8.40**	**7.66**	**8.06**
IDS	10317S002	SPIA	1993:006	1999:179			4.76
	10317S004	SPIB	1999:208	2003:224	6.95	6.59	2.56
	10317S005	SPJB	2003:258	2014:246			6.29
	-	Concatenated	1993:006	2014:246	**6.95**	**6.59**	**6.06**
IVS	10317S003	7331	1994:278	2014:365	**8.09**	**7.75**	**7.44**

Looking at the Up velocities estimated for Ny-Ålesund (see Table 5) there is clear a consistency among the three techniques at the sub-millimeter level. This good agreement can be a consequence of a more coherent reprocessing strategy used for ITRF2014 compared to that used for ITRF2008. As it is shown in Table 6, the new IDS, IVS and IGS velocities of Ny-Alesund in ITRF2014 are more consistent with respect to the ITRF2008 ones.

This improvement can also be due to a different handling and estimation strategy of the detected discontinuities, leading to more consistent inter-technique velocities. Offset detection and estimation in fact still remain a critical issue in order to further reduce offset-related velocity biases.

The harmonic analysis carried out for the Ny-Ålesund site shows some differences in the detected periodic signals, for this station we have also compared the signal phase. Results indicate that the annual component was not detected in the IVS data, whereas it was detected in the IDS and IGS data with a similar period (361.4 and 364.9 days), amplitude (4.4 and 4.0 mm), and phase (44.8 and 52.8 doy). An annual pattern can be observed in recent IVS data, apparently after 2005, but the detected signal has been rejected due to a SNR lower than 3.

7. Conclusions

Comparison and combination of space geodetic techniques contributing to the realization of the ITRF are today still challenging and very demanding to obtain reliable and coherent ITRF products. IDS, IVS and IGS Up component time series derived from the official solutions submitted to calculate new ITRF2014 have been analyzed and compared in this work. At this aim, a new approach to model time series, overcoming limitations of frequently used linear or multilinear models, has been used. The main characteristics and algorithms have been described together with main achievements. The method has proven to be very well suited to obtain quasi-cyclostationary residuals that have been used to apply harmonic analysis for the three space geodetic techniques. Then the method has shown to be very effective to estimate reliable velocities that have been compared at co-located stations.

The main results of the harmonic analysis show that, among the detected annual signals for the Up component time series, two of them with 14 days and 1 year (solar) period are com-

mon to all the three techniques. The second and third solar harmonics are common between GNSS and DORIS, then different spectral lines are close to the solar harmonic for some GNSS sites. GNSS draconitic harmonics were detected up to the eighth harmonic for several sites, whereas DORIS draconitic harmonics were difficult to observe because of the presence of artifacts. A signal with period 13.7±0.1 days and mean amplitude of 1.7 mm has been detected in 5.7% of IGS time series, with period 12±1 days and mean amplitude of 2.4 mm in 16% of IVS, with period of 15±1 days and mean amplitude of 6.1 mm in 18.3% of IDS. In the case of IDS time series, this signal might be related also to the solution interval of 7 days and it is close to the Nyquist period of 14 days.

Bloßfeld et al. (2016) have found in the IDS solutions submitted for ITRF2014 that 48% of all the station residual time series contain signal with a 14 day period. This period of about 14 days might be related to tide model errors in the fortnightly frequency band (13.6, 14.2 and 14.8 days) as it is the case of the IGS products (Ray et al., 2013). Ray and Erofeeva (2014) make clear that the IERS2010 model is deficient with respect to current tidal modeling and developed an improved model for the long-period variations in LOD (Length of Day). All the techniques need to account for these tidal variations in Earth rotation (which include harmonics near Moon fortnightly) to correctly model the rotation angle of the Earth (UT1) in order to transform from the inertial to the body-fixed frames. The tide models (GOT00.2, NAO.99b and FES2004) give for Mf amplitudes lower than 2 mm (Scherneck HG, personal communication), that can explain this effect only partially since the amplitude of the 14 days signal in the IDS time series is about 6 mm.

Griffiths and Ray (2013) suggest that aliasing of sub-daily tide constituents in daily GNSS solutions can produce signals at various periods, including 14 days. Scherneck HG (personal communication) indicates also as a possible cause of this effect the beating between Moon and Solar semidiurnals M2 and S2. In the case of the IDS weekly solution, errors could propagate from a diurnal tidal signal to longer periods, due to the fact that many of the DORIS analysis centers (IGN, INA, GOP, ESA) analyze the data by using daily arcs.

In Section 5 we have discussed how for the annual and semi-annual term, tidal and draconitic effects must be considered as contributing to the seasonal term in the GNSS time series. In Figure 6 are clearly visible several groups of mutually aliasing signals. The periods in days of the most evident solar, draconitic and tidal groups are 91.3, 87.8, 81.7 (~3 months), 121.8, 117.1, 122.6 (~4 months), 182.6, 175.6, 163.4 (semi-annual) and 365.3, 351.2, 354.1 (annual). As a consequence of their superimposition, an apparently seasonal signal could be a convolution of satellite draconitic effects as well as site-specific not modeled loading effects (Atmosphere loading and Hydrology loading), with a beating amplitude. Because of this aliasing effect, we need quite long time series to separate the solar, draconitic and tidal contributes, therefore we recommend particular care to infer e.g. regional variations in surface hydrology.

In addition to the research of common residual signatures in the Up component of the IDS, IVS and IGS time series we have also estimated the long-term behavior and velocities for the vertical and the horizontal components of the sites where the three techniques are co-located.

We determined coherent results for all the 12 sites. Anyway some hints need to be mentioned for the following sites: Canberra, Fairbanks, Syowa and Yarragadee. The first 3 sites in fact show larger STD with respect to other stations that may be explained considering that poor time series data (e.g., short data span, lack of data, few observations) are available for these sites. In Yarragadee the VLBI results for the velocity along the vertical component are not

consistent with those of DORIS and GNSS (which are consistent). We calculated the velocity on different time periods for Yarragadee's VLBI time series, and we determined that it changes significantly according to the considered time span. The time series is quite sparse and it seems to stabilize only after 2014, therefore we expect a more reliable estimate of the velocity when a long time series will be available.

Furthermore, among the 12 co-located stations, we show all the results obtained step by step during the time series processing for Ny-Ålesund site. The IDS, IVS, and IGS time series have quasi-cyclostationary residuals with respect to the long-term model. IDS and IGS have more evident periodic signals and heteroskedasticity, whereas more noisy and sparse data are present in IDS. The velocities are coherent for all the techniques. The estimated periodic signals exhibit good agreement in frequency, amplitude, and phase.

In summary examining time series obtained by ITRF2014 input solutions we have found a good agreement among all the three techniques, even if as we have explained in Section 2, being single technique solutions, the coordinates and residual signals can be datum dependent. To overcome this influence we plan to apply the same approach on ITRF2014 output time series which will be calculated in the same datum. We also would like to complete the comparison including also ILRS time series and extending the study to the horizontal components of all the sites belonging the four space geodetic techniques that have contributed to ITRF2014 realization.

8. Acknowledgements

The authors wish to thank Guilhem Moreaux (Collecte Localisation Satellites, France), Sabine Bachman and Linda Messerschmitt (BKG, Germany), and Paul Rebischung (IGS) for providing the time series coordinate intra-technique combined solutions calculated for ITRF2014 for the DORIS, VLBI and GNSS sites, respectively. We also thank them for their useful information and discussions on how the input time series for ITRF2014 were calculated. The authors also want to thank the anonymous reviewers and the editors of this issue for their constructive comments on the manuscript.

9. References

Albertella, A., Betti, B., Sansò, F., Tornatore, V., Real Time and Batch Navigation solutions: alternative approaches, Bollettino Società Italiana di Fotogrammetria e Topografia, N. 4/2005, Cagliari, ISSN 1721-971X, pp. 85-102, http://sifet.org/sifet/index.php/pubblicazioni/item/182-pubblicazioni-bolletino-sifet-eng, 2005.

Altamimi, Z., Collilieux, X., Legrand, J., Garayt, B., Boucher, C., ITRF2005: a new release of the international terrestrial reference frame based on time series of station positions and earth orientation parameters, J. Geophys. Res. 112 (B09401), doi:10.1029/2007JB004949, 2007.

Altamimi, Z., Collilieux, X., Métivier, L., ITRF2008: an improved solution of the International Terrestrial Reference Frame, J. Geodesy 85:457-473, doi:10.1007/s00190-011-0444-4, 2011.

Altamimi, Z., Collilieux, X., Métivier, L., ITRF Combination: Theoretical and practical considerations and lessons from ITRF2008 in Z. Altamimi and X. Collilieux (eds.), Reference Frames for Applications in Geosciences, IAG Symp. Ser. 138, 7-11, doi:10.1007/978-3-642-32998-2_2, 2013.

Bachmann, S., Thaller, D., Roggenbuck, O., Lösler, M., IVS contribution to ITRF2014, J Geod, doi: 10.1007/s00190-016-0899-4, 2016.

Blewitt, G. & Lavallée, D., Effect of annual signals on geodetic velocity, J. Geophys. Res., 107(B7), 2145, doi:10.1029/2001JB000570, 2002.

Bloßfeld, M., Seitz, M., Angermann, D., Moreaux, G., Quality assessment of IDS contribution to ITRF2014 performed by DGFI-TUM, Adv. Space Res., doi:10.1016/j.asr.2015.12.016, in Press, 2016.

Collilieux X., Altamimi Z., Coulot D., Ray J. & Sillard P., Comparison of VLBI, GPS, SLR height residuals from ITRF2005 using spectral and correlation methods. J. Geophys. Res., Vol. 112, B12403, doi:10.1029/2007JB004933, 2007.

Commandeur J. J. F. and Koopman S. J., An Introduction to State Space Time Series Analysis,.Oxford University Press, 2007

Ding, X. L., Zheng, D. W., Dong, D. N., Ma, C., Chen, Y. Q., Wang, G. L., Seasonal and secular positional variations at eight co-located GPS and VLBI stations, J. Geodesy, 79, 71– 81, doi:10.1007/s00190-005-0444-3, 2005.

Doodson, A.T., The harmonic development of the tide-generating potential, Proceedings of the Royal Society of London, Series A, Vol. 100, n. 704, pp. 305-329, http://www.jstor.org/stable/93989, 1921.

Gardner, A. Napolitano, L. Paura, Cyclostationarity: half a century of research, Signal Processing, 86 (4) pp. 639–697, 2006

Gazeaux, J., Williams, S., King, M., Bos, M., Dach, R., Deo, M., Moore, A.W., Ostini, L., Petrie, E., Roggero, M., Teferle, F.N., Detecting offsets in GPS time series: first results from the Detection of Offsets in GPS Experiment, J. Geophys. Res., Solid Earth, Online ISSN: 2169-9356, doi:10.1002/jgrb.50152, 2013.

Griffiths, J., Ray, R., Sub-daily alias and draconitic errors in the IGS orbits, GPS solutions, 14, 413-422, doi: 10.1007/s10291-012-0289-1, 2013.

Hefty, J., The permanent Modra-Piesok GPS station Modra-Piesok and its long-term and short-term stability, Slovak Journal of Civil Engineering, IX (1-2), 2001.

Johansson, J.M., Davis, J.L., Scherneck, H.G., Milne, G.A., Vermeer, M., Mitrovica, J.X., Bennett, R.A., Jonsson, B., Elgered, G., Elosegui, P., Koivula, H., Poutanen, M., Ronnang, B., Shapiro, I.I., Continuous GPS measurements of postglacial adjustments in Fennoscandia – 1. Geodetic results, J. Geophys. Res., Solid Earth 107(B8), 2157, doi:10.1029/2001JB000400, 2002.

Kierulf, H.P., Pettersen, B.R., MacMillan, D.S., Willis, P. , The kinematics of Ny-Ålesund from space geodetic data, J. of Geodynamics, 48(1), p.37-46. Publisher: Elsevier, Oxford, United Kingdom, ISSN: 0264-3707, doi:10.1016/j.jog.2009.05.002, 2009.

Kleijer, F., Time-series-analysis of the daily solutions of the AGRS.NL reference stations. Proc. of the IAG Symposia; Vertical Reference Systems, Cartagena, Colombia, 20-23 February 2001, vol. 124: 60-65, ISBN: 978-3-642-07701-2, doi: 10.1007/978-3-662-04683-8_13, 2002.

Langbein, J. & Johnson, H., Correlated errors in geodetic time series: Implications for time-dependent deformation, J. Geophys. Res.,102(B1), 591– 603, doi: 10.1029/96JB02945, 1997.

Mao A., Harrison, C. G. A., Dixon, T. H., Noise in GPS coordinate time series, J. Geophys. Res., 104, 2797– 2816, doi: 10.1029/1998JB900033, 1999.

Mignard, F., FAMOUS, frequency analysis mapping on usual sampling, Technical report, Obs. de la Cote d'Azur Cassiopé, Nice, France, 2005.

Moreaux G., Lemoine F. G., Capdeville H., Kuzin S., Ottend M., Štěpánek P., Willis P., Ferrage P., The International DORIS Service contribution to the 2014 realization of the International Terrestrial Reference Frame, Adv. Space Res., doi: 10.1016/j.asr.2015.12.021, 2016.

Ostini, L., Dach, R., Meindl, M., Schaer, S., Hugentobler, U., FODITS: A New Tool of the Bernese GPS Software to Analyze Time Series, EUREF 2008 Symposium, Brussels, http://www.epncb.oma.be/_documentation/papers/eurefsymposium2008/fodits_a_new_tool_of_the_bernese_gps_software.pdf, 2008.

Pearlman, M. R., Ma, C., Noll, C., Pavlis, E. C., Schuh, H., Schöne, T., Barzaghi, R., Kenyon, S., The GGOS Bureau of Networks and Observations and an Update on the Space Geodesy Networks (Geophysical Research Abstracts, Vol. 17, EGU2015-7420), General Assembly European Geosciences Union (Vienna 2015), 2015

Perfetti, N., Detection of station coordinate discontinuities within the Italian GPS Fiducial Network, J. Geodesy 80(7):381-396, doi:10.1007/s00190-006-0080-6, 2006.

Petrov, L., Ma, C., Study of harmonic site position variations determined by very long baseline interferometry, J. Geophys. Res., 108(B4), 2190, doi:10.1029/2002JB001801, 2003.

Ray, J., Altamimi, Z., Collilieux, X., van Dam, T., Anomalous harmonics in the spectra of GPS position estimates, GPS Sol. (2008) 12:55–64, doi:10.1007/s10291-007-0067-7, 2008.

Ray, J., Griffiths, J., Collilieux, X., Rebischung, P., Subseasonal GNSS positioning errors, Geophys. Res. Lett. 40(22): 5854–5860, doi:10.1002/2013GL058160, 2013

Ray, R.D., Erofeeva, S.Y., Long-period tidal variations in the length of day, J. Geophys. Res. Solid Earth, 119:1498–1509, doi:10.1002/2013JB010830, 2014.

Rebischung, P., Garayt, B., Altamimi, Z., Collilieux, X., Combination of the IGS repro2 terrestrial frames, poster presentation at the 2015 European Geosciences Union, http://acc.igs.org/repro2/Poster_EGU2015.pdf, 2015.

Roggero, M., Discontinuity detection and removal from data time series, in VII Hotine-Marussi Symposium on Mathematical Geodesy, Proceedings of the Symposium in Rome, 6-10 June, 2009, IAG Symp. Ser. 137:407-421, ISBN: 978-3-642-22077-7, doi:10.1007/978-3-642-22078-4, 2012.

Roggero, M., Extensive analysis of IGS REPRO1 coordinate time series, in VIII Hotine-Marussi Symposium on Mathematical Geodesy, Proceedings of the Symposium in Rome, 17-21 June, 2013, IAG Symp. Ser. 142:240-249, ISBN: 978-3-319-24548-5, doi:10.1007/1345_2015_58, 2016.

Scargle, J. D., Studies in astronomical time series analysis. II. Statistical aspects of spectral analysis of unevenly spaced data, Astrophys. J., 263, 835– 853, doi: 10.1086/160554, 1982.

Seitz, M., Angermann, D., Bloßfeld, M., Gerstl, M., Schmid, R., 2014 ITRS realization of DGFI: DTRF2014, presented at European Geosciences Union General Assembly, http://www.dgfi.tum.de/media/jahresbericht/posters/d8330f857a17c53d217014ee776bfd50.pdf, 2015.

Tesmer, V., Steigenberger, P., Rothacher, M., Boehm, J., Meisel, B., Annual deformation signals from homogeneously reprocessed VLBI and GPS height time series. J. Geodesy 83:973–988, doi: 10.1007/s00190-009-0316-3, 2009.

Titov, O., Yakovleva, H., Seasonal variation in radial components of VLBI stations, Astron. Astrophys. Trans., 18(4):591– 603, doi: 10.1080/10556790008208164, 2000.

Tornatore, V. & Cazzaniga, N., GPS-aided inertial navigation algorithms: new approaches, Int. J. Pure and App. Math. (IJPAM), 51(2):171-179, ISSN 1311-8080, 2009.

Valette, J.J., Lemoine, F.G., Ferrage, P., Yaya, P., Altamimi, Z., Willis, P., Soudarin, L., IDS contribution to ITRF2008, in: DORIS: precise orbit determination and applications to the earth sciences, Adv. Space Res. 46(12): 1614–1632, doi:10.1016/j.asr.2010.05.029, 2010.

Willis, P., Gobinddass, M.L., Garayt, B., Fagard, H., Recent improvements in DORIS data processing in view of ITRF2008, the ignwd08 solution, IAG Symp. Ser., 136, 43-49, doi:10.1007/978-3-642-20338-1_6, 2012.

Williams, S.D.P., The effect of coloured noise on the uncertainties of rates estimated from geodetic time-series, J. Geodesy 76 (9-10): 486-494, doi: 10.1007/s00190-002-0283-4, 2003.

Woppelmann, G., Letretel, C., Santamarìa, A., Bouin, M.N., Collilieux, X., Altamimi, Z., Williams, S., Martìn Mìguez, B., Rates of sea level change over the past century in a geocentric reference frame, Geophys. Res. Letters 36 (L12607), doi:10.1029/2009GL038720, 2009.

Yaya, P., & Tourain, C., Impact of DORIS ground antennas environment on their radio signal quality, Adv. Space Res. 45(12): 1455–1469, doi:10.1016/j.asr.2010.01.031, 2010.